PERGAMON

Solid State Communications 121 (2002) 99–102

solid state communications

www.elsevier.com/locate/ssc

Calculated de Haas-van Alphen data and plasma frequencies of MgB_2 and TaB_2

S. Elgazzar[a,b], P.M. Oppeneer[a], S.-L. Drechsler[a,*], R. Hayn[a], H. Rosner[c]

[a]*Institut für Festkörper- und Werkstofforschung, P.O. Box 270016, D-01171 Dresden, Germany*
[b]*Department of Physics, Faculty of Science, Menoufia University, Shebin El-Kom, Egypt*
[c]*Department of Physics, University of California, Davis, CA 95616, USA*

Received 12 October 2001; received in revised form 12 October 2001; accepted 29 October 2001 by P. Dederichs

Abstract

The de Haas-van Alphen frequencies as well as the effective masses for a magnetic field parallel to the crystallographic $\vec{c}$ direction are calculated within the local spin density approximation for MgB_2 and TaB_2. In addition, we analyze the plasma frequencies computed for each Fermi surface sheet. We find a large anisotropy of Fermi velocities in MgB_2 in contrast to the nearly isotropic behavior in TaB_2. © 2002 Elsevier Science Ltd. All rights reserved.

PACS: 71.18.+y; 74.70.Ad; 74.25.Jb

Keywords: A. Superconductors; C. Band structure; D. Spin–orbit effects

Due to the unexpected discovery of superconductivity in MgB_2 [1] with surprisingly high transition temperature $T_c \sim 40$ K, the clarification of its electronic structure has raised considerable interest. Band structure calculations within the density-functional theory [2–8] revealed four sheets of the Fermi surface of MgB_2 with a remarkable high anisotropy of Fermi velocities for σ-holes. That anisotropy is important to explain the significant anisotropy of the upper critical field $H_{c2}(T)$ in terms of a two-band Eliashberg model [6–8]. The relatively high value of $H_{c2}(0)$ is related to the strong electron–phonon interaction of the σ-holes on the tube-like Fermi surface sheets [8]. The details of the electronic structure may be important for precise understanding of the pairing mechanism, like, by comparing the calculated 'undressed' electronic effective mass with its actual enhanced value due to the electron–phonon coupling. On the other hand, it would be interesting to compare MgB_2 with related isostructural compounds having much lower transition temperatures or even show no superconductivity at all. We choose here TaB_2 for which band structure calculations had been reported recently [9–11] and for which single crystals can be produced [12]. It should be noted that stoichiometric TaB_2 is non-superconducting (at least down to 1.5 K [9,13,14]) and another phase, unidentified yet, should be responsible for the observed superconductivity with a T_c of 9.5 K [15].

A detailed insight into the electronic structure can be gained from de Haas-van Alphen (dHvA) measurements. Unfortunately, we are not aware of any dHvA experiments for MgB_2 or TaB_2. In an attempt to initiate possible experiments, we provide here dHvA frequencies and effective masses for the two materials under consideration. From that data, one can extract information about the Fermi velocities averaged over the extremal orbits. We also discuss the possible enhancement of the effective masses by the electron–phonon coupling which is expected to be quite different for the two materials. Information about the Fermi velocities can also be obtained by means of the plasma frequencies detectable from the Drude part of the optical conductivity. We also compare the plasma frequencies computed for each Fermi surface sheet and find a large amount of anisotropy in MgB_2 in contrast to TaB_2.

The band structure calculations have been performed by means of the fully relativistic augmented spherical waves method [16]. We used the von Barth–Hedin parametrization of the exchange-correlation potential. A k-mesh of 148 special k-points in the irreducible Brillouin zone part was

* Corresponding author. Tel.: +49-351-4659-384; fax: +49-351-4659-490.

E-mail address: drechsler@ifw-dresden.de (S.-L. Drechsler).

0038-1098/02/$ - see front matter
PII: S0038-1098(01)00460-4

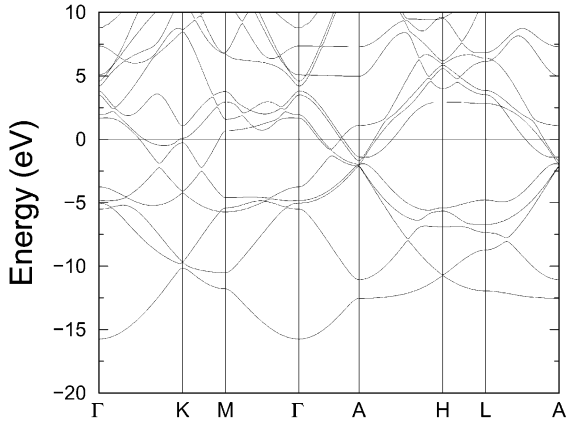

Fig. 1. The calculated energy bands of TaB_2.

chosen. Both compounds crystallize in the hexagonal space group $P6_3/mmc$ with lattice constants $a = 3.085$ Å, $c = 3.522$ Å and $a = 3.082$ Å, $c = 3.243$ Å [15] for MgB_2 and TaB_2, respectively. The resulting band structures for MgB_2 coincides completely with those published in the literature [2–8] and is not shown, the fully relativistic band structure of TaB_2 is presented in Fig. 1. We have checked our results by comparing them with the scalar relativistic full-potential local orbital method by repeating our previous calculation (MgB_2 [6–8], TaB_2 [9]) and found no remarkable difference for MgB_2. There, lifting of degeneracy due to the spin–orbit coupling in a fully relativistic calculations does not affect the band structure near the Fermi level. In contrast, the spin–orbit coupling of the Ta 5d states in TaB_2 results in differences compared to scalar relativistic calculations, especially between Γ and A (compare Figs. 1 and 3 of Ref. [9]). Although these differences did not affect the absence of superconductivity in this compound, they lead to consequences for the Fermi surface discussed later.

To predict the dHvA frequencies F for a magnetic field applied along the crystallographic $\vec{c}$ direction, we calculate the area A of any extremal orbit Ω according to

$$F = \frac{\hbar}{2\pi e}A = \frac{\hbar}{2\pi e}\int_{\Omega} \mathrm{d}^2k, \tag{1}$$

where F is given in units of the magnetic field, i.e. in kT. The effective mass of the corresponding orbit is given by:

$$m = \frac{\hbar}{2\pi}\oint \frac{\mathrm{d}k}{|\vec{v}_k|}, \qquad \text{with } \vec{v}_k = \frac{\partial \epsilon_k}{\partial \vec{k}}. \tag{2}$$

From the dHvA frequency F and the effective mass m, one can calculate the effective Fermi velocity

$$v_\mathrm{f} = \frac{1}{m}\sqrt{2\hbar e F}, \tag{3}$$

which corresponds to the hypothetical value for a circular orbit with constant $|\vec{v}_k|$. This expression is frequently used to estimate the Fermi velocity from dHvA data. Alternatively, one can also average $1/|\vec{v}_k|$ around the circumference and define

$$\tilde{v}_\mathrm{f} = \frac{\hbar L}{2\pi m} = \frac{\hbar}{2\pi m}\oint \mathrm{d}k. \tag{4}$$

Both Eqs. (3) and (4) coincide for a circular orbit. Information about the Fermi velocity is also contained in the plasma frequencies $\omega_{p,\alpha}$ ($\alpha = x(y)$ or z)

$$(\omega_{p,\alpha})^2 = \frac{e^2}{\epsilon_0}\int \frac{\mathrm{d}^3k}{(2\pi)^3}\,\delta(\epsilon_k - E_\mathrm{f})(v_{k,\alpha})^2, \tag{5}$$

where we distinguish the contributions from different Fermi surface sheets in the following (denoted by $\omega^n_{p,\alpha}$).

Let us first discuss the results for MgB_2 (Tables 1 and 2). The Fermi surface (see Fig. 1 in Ref. [7]) consists of four sheets and there are six extremal orbits for a magnetic field in the $\vec{c}$ direction. We denote them by numbers 1–3 centered around Γ and 4–6 centered around A with increasing area in each case. So one can see that orbits 1 and 4 (2 and 5) belong to the smaller (larger) tube, whereas the remaining orbits 3

Table 2
Squared plasma frequencies of MgB_2 in atomic units (Ry^2). One atomic unit for the plasma frequency corresponds to 10.94×10^5 m/s and the summed value is given for both the spin directions

FS sheet	$\omega^2_{p,x(y)}$	$\omega^2_{p,z}$	$v_{x(y)}/v_z$
1 (tube)	0.340×10^{-1}	0.065×10^{-2}	7.20
2 (tube)	0.333×10^{-1}	0.087×10^{-2}	6.17
3 (ring)	0.304×10^{-1}	0.596×10^{-1}	0.71
4 (ring)	0.812×10^{-1}	0.666×10^{-1}	1.10
All	0.3578	0.2555	1.18

Table 1
Calculated dHvA data of MgB_2

Orbit	$F(kT)$	A (nm^{-2})	A/A_{BZ} (%)	m/m_0	v_f (m/s)	$\tilde{v}_\mathrm{f}$ (m/s)
1	0.991	9.46	1.98	0.254	7.91×10^5	8.47×10^5
2	2.305	21.99	4.60	0.313	9.79×10^5	1.05×10^6
3	32.879	313.70	65.56	1.699	6.81×10^5	7.15×10^5
4	2.155	20.56	4.30	0.550	5.39×10^5	5.77×10^5
5	4.309	41.11	8.59	0.612	6.84×10^5	7.33×10^5
6	30.195	288.09	60.21	0.924	1.20×10^6	1.28×10^6

Table 3
Calculated dHvA data of TaB_2

Orbit	$F(kT)$	A (nm^{-2})	A/A_{BZ} (%)	m/m_0	v_f (m/s)	$\tilde{v}_f$ (m/s)
1	2.081	19.85	4.14	0.221	1.32×10^6	1.41×10^6
2	2.985	28.44	5.93	0.356	9.79×10^5	1.05×10^6
3	8.398	80.01	16.69	0.677	8.64×10^5	9.26×10^5
4	13.262	126.36	26.36	0.558	1.32×10^6	1.41×10^6
5	1.051	10.01	2.09	0.236	8.69×10^5	8.91×10^5
6	1.151	10.96	2.29	0.632	3.39×10^5	3.65×10^5

and 6 are rather large and belong to the ring-like parts of the Fermi surface. The electrons on orbit 6 have the largest Fermi velocity and v_f of orbit 3 is smaller compared to that of orbit 6 due to the larger effective mass. The electrons on the tubes are slow in general, with the minimal velocity on orbit 4. The ratio of Fermi velocities for the two different groups of electrons is roughly 2, confirming the two band model of Ref. [7]. The difference between v_f and $\tilde{v}_f$ does not exceed 7% and is remarkable only for those orbits which have a more hexagonal form than a circular one (orbit 3 is an example for a nearly circular orbit). According to the two-band model [7], we would expect a different electron–phonon mass renormalization $(1+\lambda)$ for electrons on the tubes (with $\lambda \simeq 1.2$–1.5) and on the large orbits 3 and 6 ($\lambda \simeq 0.3$). So, the experimental determination of the effective masses by dHvA measurements and its comparison with the calculated electronic values would give important information on details of the electron–phonon coupling. The anisotropy of Fermi velocities of MgB_2 is even more visible in our calculated plasma frequencies (Table 2), which are similar to the results of Refs. [3,4]. It is another kind of anisotropy: the z-component of v_f is 6–7 times smaller than $x(y)$ components for the two tubes (sheets 1 and 2). The anisotropy ratio $v^n_{p,x(y)}/v^n_{p,z}$ ($v^n_\alpha \propto |\omega^n_{p,\alpha}|$) is much smaller for the sheets 3 and 4 and its average Fermi velocity is larger. The total plasma frequency, however, shows only a small anisotropy of 1.18 between the z and $x(y)$ components.

The anisotropy of Fermi velocities is much less pronounced in TaB_2 (Tables 3 and 4). Our fully relativistic Fermi surface coincides almost with that published in Ref. [9] and consists of three sheets. The extremal orbits are characterized as follows: numbers 1–3 are centered around the A point and correspond to the three different sheets.

Table 4
Squared plasma frequencies of TaB_2 in atomic units (Ry^2)

FS sheet	$\omega^2_{p,x(y)}$	$\omega^2_{p,z}$	$v_{x(y)}/v_z$
1	0.2037	0.2290	0.94
2	0.453×10^{-1}	0.461×10^{-1}	0.99
3	0.970×10^{-2}	0.879×10^{-2}	1.05
All	0.5175	0.5677	0.95

Orbit 4 is centered around K and orbit 5 corresponds to the small Fermi surface part in the neighborhood of K. There is one maximal orbit (number 6) with non-trivial value k_z ($0.20615\times2\pi/a$). Since Ta is a 5d element, the influence of the spin–orbit coupling is more pronounced in TaB_2 than in MgB_2. With respect to the scalar relativistic calculations [9], we find two differences that affect the Fermi surface. First, a splitting of bands along the high symmetry direction Γ–A, which leads to lifting of band degeneracy at the Fermi level. Second, also at the K-point, a small band shift occurs. The first spin–orbit modification of the Fermi surface makes one Fermi sheet disjointed along Γ–A. The calculated areas, effective masses and Fermi velocities of TaB_2 are collected in Table 3 and one can see that any kind of anisotropies of Fermi velocities is much smaller than for MgB_2. According to the calculation of the electron–phonon coupling constants [9], we would expect a rather small renormalization of effective masses in TaB_2 ($\lambda \simeq 0.05$–0.2) again in contrast to MgB_2. The plasma frequencies are collected in Table 4. Since there are no analogous FS sheets to the two tubes of MgB_2, we do not obtain a corresponding anisotropy in $\omega^n_{p,x(y)}$ with respect to $\omega^n_{p,z}$. This can be understood due to the loss of the quasi two-dimensionality of the B σ-states in TaB_2 due to the hybridization with the Ta 5d states.

In summary, we have calculated the dHvA frequencies and effective masses as well as the plasma frequencies of MgB_2 and TaB_2 which would be worth to investigate experimentally. The comparison of the experimental masses with our calculation could give important information on the electron–phonon coupling. According to Refs. [2,8,9], we expect remarkable differences between MgB_2 and TaB_2: large enhancement for one group of electrons in MgB_2 and a small enhancement for the other electrons in MgB_2 as well as in TaB_2. We found a remarkable anisotropy of Fermi velocities in superconducting MgB_2 which is in contrast to the more isotropic behavior of non-superconducting TaB_2.

Acknowledgements

We thank S.V. Shulga, H. Eschrig, M. Richter, V.D.P. Servedio, and other members of the solid state theory

group at the IFW Dresden for discussions. This work was supported by the Egyptian Ministry of Higher Education and Scientific Research and DAAD (individual grant to H.R.), ONR Grant No. N00017-1-0956 and the DFG, SFB 463.

References

[1] J. Nagamatsu, N. Nakagawa, T. Muranaka, Y. Zenitani, J. Akimitsu, Nature 410 (2001) 63.
[2] J.M. An, W.E. Pickett, Phys. Rev. Lett. 86 (2001) 4366.
[3] J. Kortus, I.I. Mazin, K.D. Belashchenko, V.P. Antropov, L.L. Boyer, Phys. Rev. Lett. 86 (2001) 4656.
[4] A.Y. Liu, I.I. Mazin, J. Kortus, Phys. Rev. Lett. 87 (2001) 087005.
[5] Y. Kong, O.V. Dolgov, O. Jepsen, O.K. Andersen, Phys. Rev. B 64 (2001) 0250501.
[6] G. Fuchs, S.-L. Drechsler, S.V. Shulga, K.-H. Müller, A. Handstein, K. Nenkov, H. Rosner, in: A. Narlikar (Ed.), Studies of High-Temperature Superconductors, vol. 41, Nova Science Publishers, Commack, NY, 2001 in press.
[7] S.V. Shulga, S.-L. Drechsler, H. Eschrig, H. Rosner, W.E. Pickett, cond-mat/0103154, 2001.
[8] H. Rosner, J.M. An, W. Ku, M.D. Johannes, R.T. Scalettar, W.E. Pickett, S.V. Shulga, S.-L. Drechsler, H. Eschrig, W. Weber, A.G. Eguiluz, in: A. Narlikar (Ed.), Studies of High-Temperature Superconductors, vol. 38, Nova Science Publishers, Commack, NY, 2001 in press.
[9] H. Rosner, W.E. Pickett, S.-L. Drechsler, A. Handstein, G. Behr, G. Fuchs, K. Nenkov, K.-H. Müller, H. Eschrig, Phys. Rev. B 64 (2001) 144516.
[10] I.R. Stein, A.L. Ivanovski, cond-mat/0109445, 2001.
[11] P.P. Singh, cond-mat/0104580, 2001.
[12] S. Otani, M.M. Korsukova, T. Miksuhashi, J. Cryst. Growth 194 (1998) 430.
[13] L. Leyarovska, E. Leyarovska, J. Less Common Metals 67 (1979) 249.
[14] V.A. Gasparov, N.S. Sidorov, I.L. Zvor'kova, M.P. Kulakov, JEPT Lett. 73 (2001) 532.
[15] D. Kaczorowski, A.J. Zaleski, O.J. Zogal, J. Klamut, cond-mat/0103571, 2001.
[16] A.R. Williams, J. Kübler, C.D. Gelatt, Phys. Rev. B 19 (1979) 6094.